Desalination and Water Treatment
www.deswater.com
doi: 10.5004/dwt.2023.29600

295 (2023) 191–204
May

Simulation and optimization of supercritical water oxidation processes

Guodong Yu, DeDong Hu*

College of Electromechanical Engineering, Qingdao University of Science and Technology, Qingdao 266100, China, email: hudedong@126.com (D.D. Hu)

Received 19 December 2022; Accepted 30 April 2023

ABSTRACT

Supercritical water oxidation technology (SCWO) is an environmentally friendly and excellent performance technology in treating refractory organic wastes. High treatment cost is the main drawback restricting SCWO large-scale application. The optimization of the SCWO process is a critical concern for the industrialization of SCWO technology. In order to reduce the cost, in this work four SCWO wastewater treatment processes (treatment capacity of 2 t/h) with or without high pressure energy recovery and using air or liquid oxygen as oxidant were firstly constructed. And the processes were simulated and optimized with the exergy efficiency as the objective function using the response surface method and Aspen Plus software. Lastly, the economic evaluation of SCWO processes was carried out. The optimized SCWO process with liquid oxygen as oxidant and without the high-pressure energy recovery was obtained, and the optimized parameters were temperature 849.83 K, the excess oxygen coefficient 1 and the pressure 25.4 MPa. The process has the second highest exergy efficiency of 38% and the process has the lowest capital requirements and equipment cost. The results above can provide theoretical support for the industrialization of SCWO technology.

Keywords: Supercritical water oxidation processes; Simulation; Optimization; Exergy efficiency; Aspen Plus

1. Introduction

With the worsening of environmental problems, environmental pollution has become an issue of universal concern for human society. The supercritical water oxidation (SCWO) technology [1] which uses the unique physical–chemical properties of water above the critical point (374.2°C and 22.1 MPa) has attracted the attention of numerous researchers especially in treating high concentration and refractory organic waste owing to its advantages of treating wastewater quickly, efficiently and environmentally [2,3]. Although SCWO shows excellent effects in waste treatment, certain inherent drawbacks, such as salt-plugging corrosion and high costs, are still the obstacles to its commercial application [4]. Liao et al. [5] studied a pilot-scale SCWO system with a novel jet reactor. The results showed that the reaction temperature and wastewater concentration had a positive influence on reducing cost. Belén García-Jarana et al. [6] studied a pilot-scale SCWO-SCWG system. The results showed that the high concentration organic wastewater SCWO treatment product is beneficial for the generation of hydrogen from isopropanol solution. Xu et al. [7] proposed the first SCWO pilot-scale plant for sewage sludge treatment in China. The results showed that the minimized plant operating cost depends on milder reaction conditions, lower oxygen consumption, more adequate energy recovery and more by-product income. Yang et al. [8] proposed a commercial scale concept for SCWO of sewage sludge. The results showed that the effective methods to reduce the operating cost were thermal hydrolysis treatment of sludge and methanol-assisted start-up.

The costs including equipment costs and operating costs are closely related to SCWO processes using air [9,10] or liquid oxygen [11–14] as oxidant and high temperature heat

* Corresponding author.

energy [15,16] and using or not using high pressure energy recovery [17]. It is important to increase the SCWO process exergy efficiency to reduce cost. Bernrjo et al. [18] studied the SCWO process of coal using air as oxidant, preheating and power generation. The results showed that the energy efficiency of process with reheating cycle was 8% higher than the conventional process. Marias et al. [19] studied the SCWO process of wastewater with oxygen as oxidant, preheating and energy recovery. The results showed that the heat released from the oxidation of organic matter should be recovered by heat energy. Huang et al. [20] researched the influence of hydrothermal flame method on the SCWO exergy efficiency where increasing the reactor temperature was beneficial to improve the system exergy efficiency. Zhang et al. [21] studied the exergy efficiency of the black liquor SCWO process was 13.28%. Liang et al. [22] studied the exergy efficiency of the black liquor SCWO process at temperatures ranging from 873.15 to 1,073.15 K was 17.69%–18.27%. Power generation and pre-heating were used to recover heat energy. Luo et al. [23] studied the process combined with organic Rankine cycle and organic wastewater SCWO and the process exergy efficiency was 34.54%. Sharan et al. [24] studied the recompression Rankine cycle used to recover SCWO desalination process energy and the process thermoelectric conversion efficiency was 37.8%. Xi et al. [25] studied the combined organic Rankine cycle and SCWO process system with the exergy efficiency of 22.45%. However, there is no comprehensive study on the influence of SCWO process parameters on exergy efficiency.

In this paper, the SCWO process is systematically analyzed with different oxidants and energy recovery. In order to reduce the cost and improve the process exergy efficiency, four SCWO wastewater treatment processes using or not using high pressure energy recovery and using air or liquid oxygen as oxidant are constructed, simulated and optimized with the exergy efficiency as the objective function using the surface response method, Aspen Plus software and economic evaluation, and the optimal SCWO process is obtained in this paper.

2. SCWO process construction

To optimize the SCWO process, four SCWO wastewater treatment processes were constructed based on recovering high pressure energy or not and the air or liquid oxygen as oxidant.

As can be seen in Fig. 1, air is used as the oxidant without recovering high pressure energy in Process 1. The wastewater was pumped by a high-pressure plunger pump, preheated by the preheater and sent to the SCWO reactor. The reactor was heated reaching to the anticipated temperature by electromagnetic heater. The air was compressed by the compressor to preset pressure and then mixed with the wastewater in the reactor. The reaction product was separated from the inorganic salt in the reactor and then entered the evaporator to recover the excess heat energy. The waste gas was injected into the preheater to preheat the wastewater.

As can be seen in Fig. 2, air is used as the oxidant with recovering high pressure energy in Process 2. The wastewater was pumped by the high-pressure plunger pump, preheated by the preheater and sent to the SCWO reactor.

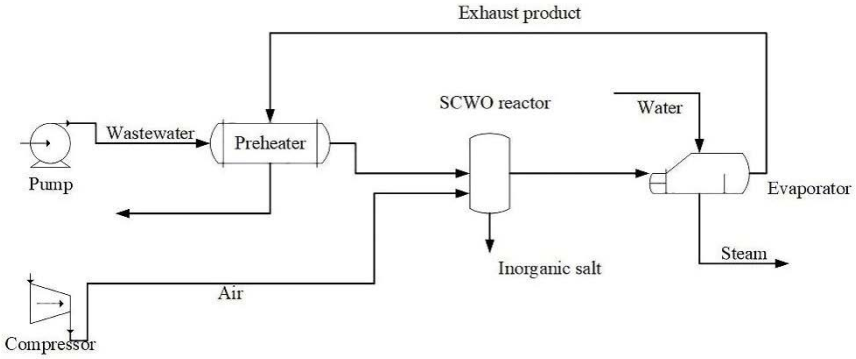

Fig. 1. Schematics diagram of SCWO wastewater treatment Process 1.

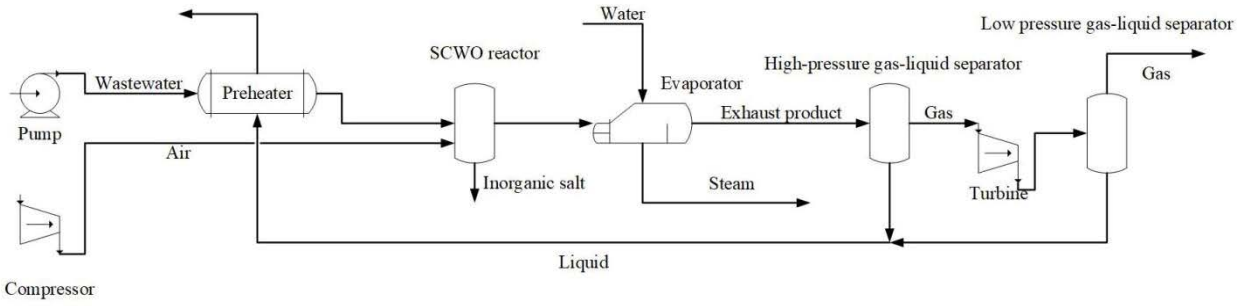

Fig. 2. Schematics diagram of SCWO wastewater treatment Process 2.

The reactor was heated reaching to the anticipated temperature by electromagnetic heater. The air was compressed by the compressor to preset pressure and then mixed with wastewater in the reactor. The reaction product was separated from the inorganic salt in the reactor and then entered the evaporator to recover the heat energy. Finally, the exhaust effluent was separated into gas–liquid two-phase in the high-pressure gas–liquid separator and the gas phase was transmitted to the turbine to recover pressure energy. The turbine outlet pressure reached an anticipated pressure. The turbine exhaust was further separated into gas–liquid two-phase in the low-pressure gas–liquid separator. The liquid phase from the two gas–liquid separators was injected into the preheater together to preheat the wastewater.

As can be seen in Fig. 3, liquid oxygen is used as the oxidant without recovering high pressure energy in Process 3. The wastewater was pumped by the high-pressure plunger pump, preheated by the preheater and sent to the SCWO reactor. The reactor was heated reaching to the anticipated temperature by electromagnetic heater. Liquid oxygen was pumped by a liquid oxygen pump to preset pressure and then mixed with the wastewater in the reactor. The reaction product was separated from the inorganic salt in the reactor and then entered the evaporator to recover the heat energy. The waste gas was injected into the preheater to preheat the wastewater.

As can be seen in Fig. 4, liquid oxygen is used as the oxidant with recovering high pressure energy in Process 4. The wastewater was pumped by the high-pressure plunger pump, preheated by the preheater and sent to the SCWO reactor. The reactor was heated reaching to the anticipated temperature by electromagnetic heater. Liquid oxygen was pumped by a liquid oxygen pump to preset pressure and then mixed with the wastewater in the reactor. The reaction product was separated from the inorganic salt in the reactor, and then entered the evaporator to recover the heat energy. Finally, the exhaust effluent was separated into gas–liquid two-phase in the high-pressure gas–liquid separator, and the gas phase was transmitted to the turbine to recover pressure energy. The turbine outlet pressure reached an anticipated pressure. The turbine exhaust was further separated into gas–liquid two-phase in the low-pressure gas–liquid separator. The liquid phase from the two gas–liquid separators was injected into the preheater together to preheat the wastewater.

3. SCWO process modelling

As can be seen in Figs. 5–8, four SCWO wastewater treatment processes were modeled in Aspen Plus with steady-state simulations. The air compressor and turbine were simulated by the compressor model Compr, in which the stream is isentropic. The steam generator that generated steam at 6MPa and 275.45°C and preheater were simulated by the counter-current heat exchanger model HeatX. The high-pressure gas–liquid separator and low-pressure

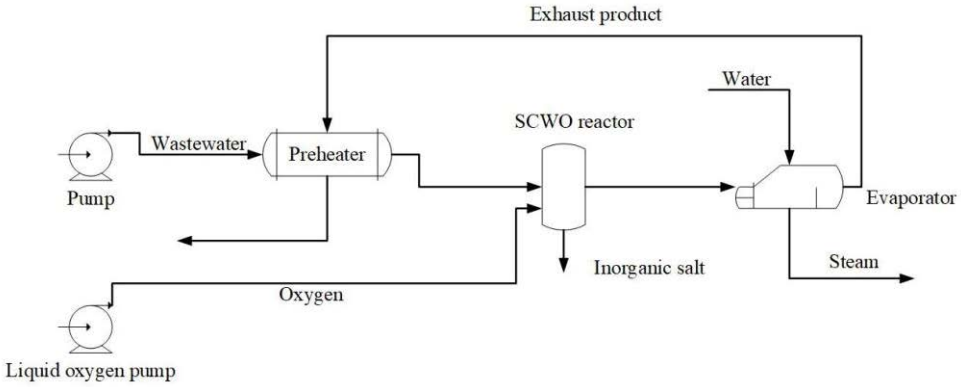

Fig. 3. Schematics diagram of SCWO wastewater treatment Process 3.

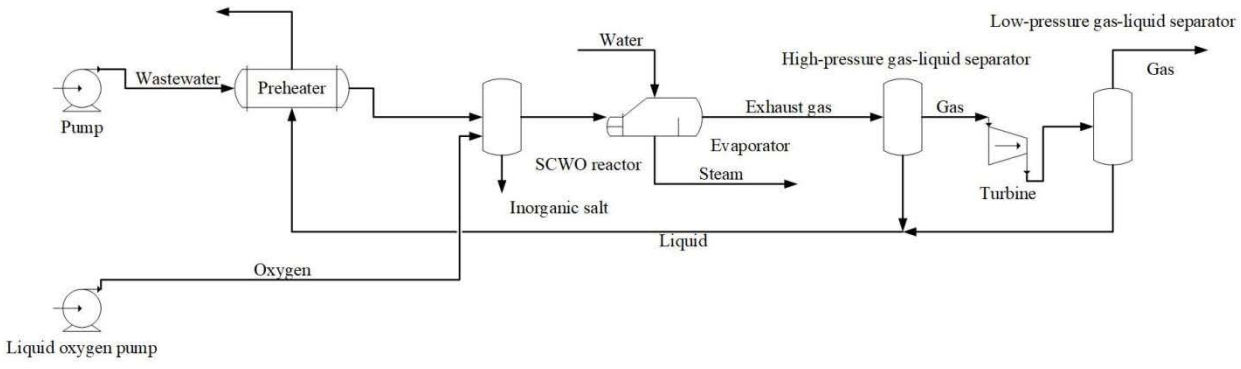

Fig. 4. Schematics diagram of SCWO wastewater treatment Process 4.

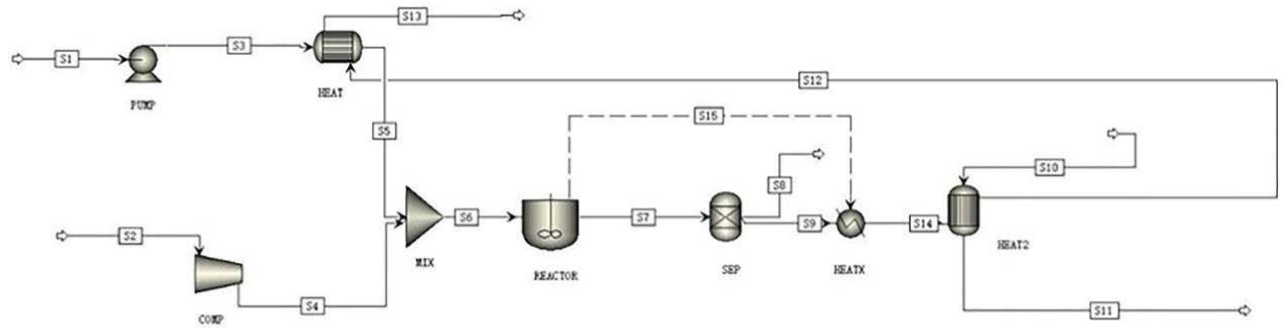

Fig. 5. The Aspen Plus simulation flowsheet for the SCWO wastewater treatment process model 1.

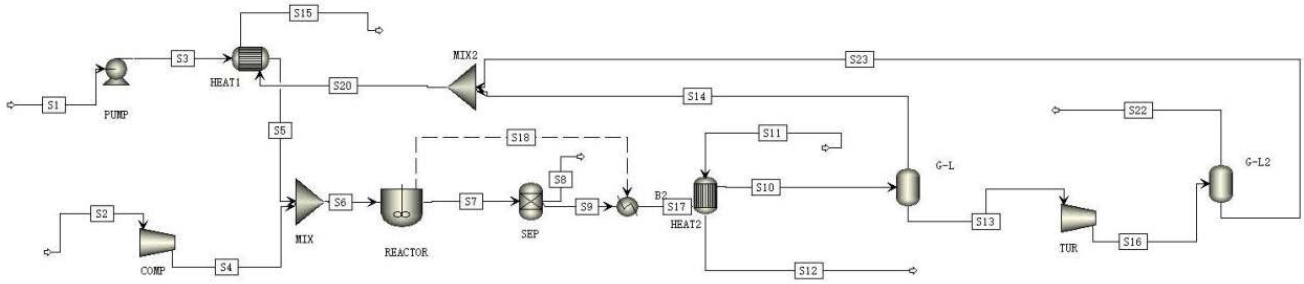

Fig. 6. The Aspen Plus simulation flowsheet for the SCWO wastewater treatment process model 2.

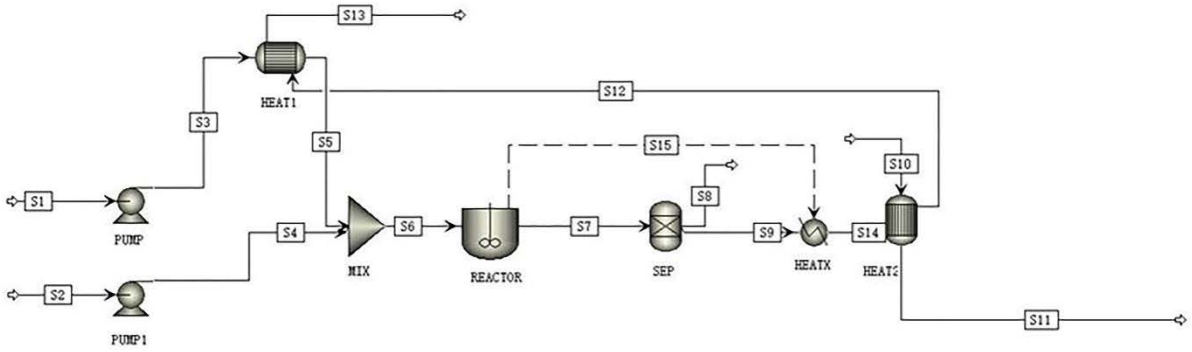

Fig. 7. The Aspen Plus simulation flowsheet for the SCWO wastewater treatment process model 4.

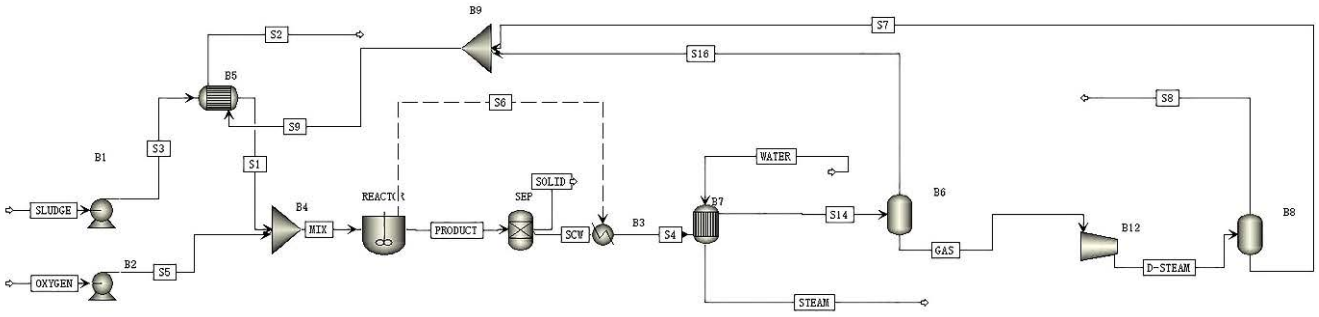

Fig. 8. The Aspen Plus simulation flowsheet for the SCWO wastewater treatment process model 4.

gas–liquid separator used to separate waste gas were simulated through the component separator model Flash2. The liquid oxygen pump and high plunger pump used to conduct adiabatic compression of liquid oxygen and wastewater were simulated through the PUMP model. The SCWO reactor was simulated by the stream mixer model MIXER, the full mixer model RCSTR, the component separator model Sep and the heater model Heater. The wastewater and oxidant

were mixed in the MIXER and then reacted in the RCSTR. The separator generated high-temperature stream separated from inorganic salts. At the same time, the Heater was used to balance the reactor heat.

4. SCWO process simulation and optimization

4.1. Design of the SCWO process simulation

In order to describe the influence of the interaction between the factors on the exergy efficiency, multiple regression analysis was performed on the basis of the each SCWO process simulation data. Box–Behnken design [25] assisted RSM Design–Expert software 10.0 was used to statistically analyze simulation data of each process. The design (Table 1) of the each SCWO process consisted of 17 runs was carried out to optimize the levels of the selected independent factors: temperature (*A*), pressure (*B*), and excess oxygen coefficient (*C*). As can be seen in Eq. (1), the response variable of the SCWO process was explained by the second-order polynomial equation with three-factorial.

$$Y = \beta_0 + \sum \beta_i x_i + \sum \beta_{ij} x_i x_j + \sum \beta_{ii} x_i^2 \quad (1)$$

where Y denotes the value of the exergy efficiency, whereas β_0, β_i, β_{ii}, and β_{ij} represent the regression coefficient for the term intercept, linear, square, and interaction effects, respectively. Also, x_i and x_j are the independent variables.

4.2. SCWO process simulation

In this paper, four SCWO processes were simulated and optimized using the response surface method and Aspen Plus software based on wastewater treating project (treatment capacity of 2 t/h). The wastewater contains 11% methanol and 3% ammonium chloride. Peng Robinson equation [26] was used as the fluid property method of wastewater, air and liquid oxygen in the process, and the reaction kinetics equations of ammonium salt (ammonia) and methanol [27,28] were simulated for SCWO reaction of wastewater. Pressure and heat losses were ignored in connecting piping and devices.

4.3. Analysis of exergy efficiency

Exergy [29] consists of physical and chemical exergy, in which the exergy value of steady flow is in Eq. (2). The enthalpy and entropy of substance are H and S. H_0, T_0 and S_0 are the enthalpy, temperature and entropy of reference conditions (298.15K, 1 atm), respectively.

$$\mathrm{Ex_{ph}} = H - H_0 - T_0\left(S - S_0\right) + 0.5\mathrm{mc}^2 + \mathrm{mgz} \quad (2)$$

The chemical exergy of methanol could be calculated by Eq. (3):

$$\mathrm{Ex_{ch3oh}} = \mathrm{Ex_{co_2}} + 2\mathrm{Ex_{h_2o}} - 1.5\mathrm{Ex_{o_2}} + H_{\mathrm{react1}} \quad (3)$$

where $\mathrm{Ex_{ch_3oh}}$, $\mathrm{Ex_{co_2}}$, $\mathrm{Ex_{h_2o}}$ and $\mathrm{Ex_{o_2}}$ are the chemical exergy of the methanol, carbon dioxide, water and oxygen, respectively. H_{react1} is the reaction heat of methanol.

The chemical exergy of ammonium chloride could be calculated by Eq. (4).

$$\mathrm{Ex_{nh4cl}} = 0.5\mathrm{Ex_{n2}} + 1.5\mathrm{Ex_{h_2o}} - 0.75\mathrm{Ex_{o_2}} + \mathrm{Ex_{hcl}} + H_{\mathrm{react2}} \quad (4)$$

where $\mathrm{Ex_{nh4cl}}$, $\mathrm{Ex_{n_2}}$, $\mathrm{Ex_{hcl}}$, $\mathrm{Ex_{h_2o}}$ and $\mathrm{Ex_{o_2}}$ are the chemical exergy of ammonium chloride, nitrogen, hydrogen chloride, water and oxygen, respectively. H_{react2} is the reaction heat of ammonium chloride.

Table 1
Exergy efficiency of four SCWO processes

Number	Temperature (°C)	Pressure (MPa)	EOC	Process 1 (%)	Process 2 (%)	Process 3 (%)	Process 4 (%)
1	500	26	2	32.10	34.65	23.56	13.47
2	550	26	1.5	37.80	37.88	35.84	24.59
3	550	26	1.5	37.80	37.88	35.84	24.59
4	550	26	1.5	37.80	37.88	35.84	24.59
5	600	28	1.5	37.98	38.01	36.11	24.68
6	550	28	2	37.96	40.16	35.22	24.61
7	500	28	1.5	31.22	31.52	24.00	12.90
8	500	26	1	29.88	27.26	24.45	12.83
9	550	24	2	37.88	40.25	35.30	25.23
10	550	28	1	37.61	34.65	36.34	24.01
11	550	26	1.5	37.80	37.88	35.84	24.59
12	600	26	1	37.89	34.98	36.72	24.65
13	550	24	1	37.73	34.85	36.37	24.63
14	500	24	1.5	31.10	31.46	23.94	13.41
15	550	26	1.5	37.80	37.88	35.84	24.59
16	600	26	2	38.13	40.37	35.68	25.26
17	600	24	1.5	37.99	38.14	36.17	25.31

The exergy efficiency of the SCWO Process could be calculated by Eq. (5).

$$\eta = \frac{W_{\text{turbine}} + Ex_{\text{steam}}}{W_{\text{pump}} + W_{\text{liquidoxygenpump}}\left(W_{\text{compressor}}\right) + \text{Ex}_{\text{ch3oh}} + \text{Ex}_{\text{nh4cl}}} \times 100\% \tag{5}$$

where W_{pump}, $W_{\text{compressor}}$ and $W_{\text{liquidoxygenpump}}$ are the electricity power input of the plunger pump, air compressor and liquid oxygen pump, respectively. W_{turbine} is the electricity power output of the turbine and Q_{steam} is the exergy value of by-product steam.

5. Results and discussions

5.1. Optimization of the SCWO processes

It can be seen from Table 1 that the exergy efficiency ranges of SCWO Processes 1–4 were 29.88%–38.13%, 27.26%–40.37%, 23.56%–36.72% and 12.83%–25.31%, respectively and the exergy efficiency values from high to low were Process 2, Process 1, Process 3 and Process 4. After applying multiple linear regressions, the polynomial models 1–4, as shown in Table 2, describing the quantitative effect of the exergy efficiency and independent factors and their first-order interaction on the response are obtained. A positive sign of the terms in models 1–4 indicated a synergistic effect, while a negative sign indicates an antagonistic effect of the response. The quality of the developed models 1–4 were evaluated based on the correlation coefficient (R^2) values. The R^2 values of 0.9965, 0.9977, 1 and 1 indicate a high degree of agreement between the quadratic models and simulation data. The analysis of variance (ANOVA) was the statistical tool which defines the significance and accuracy of developed quadratic response surface models. According to ANOVA results (Tables 3–6). The smaller the '*P*-value', the more significant was the corresponding coefficient. Four "*P*-values" were less than 0.0001 imply that those models are significant. Obviously, for SCWO Process 1, as shown in Table 3, temperature was the most significant variable for the response with the smallest '*P*-value'. However, pressure did not have an influence on the exergy efficiency with the highest *P*-value among the three variables. The same conclusion can be drawn that three parameters have significant effects in the order (temperature > excess oxygen coefficient > pressure) on the exergy efficiency. For SCWO Process 2 and 3, as shown in Tables 4 and 5, temperature and excess oxygen coefficient were both the significant variables for the response with the small '*P*-values'. But pressure did not have an influence on the exergy efficiency with the highest *P*-value among the three variables. For SCWO Process 4, as shown in Table 6, temperature, pressure and

Table 2
Exergy efficiency equation of processes

Model	Fitting equations
1	$-4.1+1.543E^{-2}A-3.254E^{-3}B+1.087E^{-1}C-3.22E^{-6}AB-1.99E^{-4}AC+4.94E^{-4}BC-1.3E^{-5}A^2+8.3E^{-5}B^2-1.56E^{-3}C^2$
2	$-4.066+1.487E^{-2}A-2.21E^{-3}B+2.144E^{-1}C-4.86E^{-6}AB-2E^{-4}AC+2.72E^{-4}BC-1.3E^{-5}A^2+8.2E^{-5}B^2-1.74E^{-2}C^2$
3	$-7.374+2.66E^{-2}A+7.03E^{-3}B+2.7E^{-5}C-3.25E^{-6}AB-1.6E^{-5}AC-9.4E^{-5}BC-2.3E^{-5}A^2-1E^{-4}B^2+2.49E^{-4}C^2$
4	$-7.083+2.566E^{-2}A-3.255E^{-3}B+6.76E^{-3}C-3.13E^{-6}AB-3.23E^{-6}AC+2.9E^{-5}BC-2.2E^{-5}A^2+6.6E^{-5}B^2+1.29E^{-4}C^2$

A-Temperature; B-Pressure; C-Excess oxygen coefficient

Table 3
ANOVA results for exergy efficiency of SCWO Process 1

Source	Sum of squares	df	Mean square	*F*-value	*P*-value
Model	0.0413	9	0.0016	220.21	<0.0001
A-Temperature	0.0096	1	0.0096	1,327.97	<0.0001
B-Pressure	3.482E-8	1	3.482E-8	0.0048	0.9466
C-EOC	0.0001	1	0.0001	15.12	0.006
AB	4.159E-7	1	4.159E-7	0.0576	0.8171
AC	0.0001	1	0.0001	13.73	0.0076
BC	9.772E-7	1	9.772E-7	0.1354	0.7237
A^2	0.0045	1	0.0045	620.99	<0.0001
B^2	4.648E-7	1	4.648E-7	0.0644	0.8069
C^2	6.426E-7	1	6.426E-7	0.0891	0.774
Residual	0.0001	7	7.215E-6		
Lack of fit	0.0001	3	0.0000		
Pure error	0.0000	4	0.0000		

R^2 = 0.9965; Adeq. precision = 39.0662; Adjusted R^2 = 0.9920; Predicted R^2 = 0.9437; CV = 0.7407%; SD = 0.0027.

Table 4
ANOVA results for exergy efficiency of SCWO Process 2

Source	Sum of squares	df	Mean square	*F*-value	*P*-value
Model	0.0203	9	0.0023	341.42	<0.0001
A-Temperature	0.0088	1	0.0088	1341.37	<0.0001
B-Pressure	1.567E-6	1	1.567E-6	0.2378	0.6407
C-EOC	0.007	1	0.007	1,064.74	<0.0001
AB	9.444E-7	1	9.444E-7	0.1433	0.7162
AC	0.0001	1	0.0001	15.2	0.0059
BC	2.964E-7	1	2.964E-7	0.045	0.8381
A^2	0.0041	1	0.0041	626.24	<0.0001
B^2	4.507E-7	1	4.507E-7	0.0684	0.8012
C^2	0.0001	1	0.0001	12.08	0.0103
Residual	0.0000	7	6.59E-6		
Lack of fit	0.0000	3	0.0000		
Pure error	0.0000	4	0.0000		

R^2 = 0.9977; Adeq. precision = 65.6624; Adjusted R^2 = 0.9948; Predicted R^2 = 0.9636; CV = 0.7088%; SD = 0.0026.

Table 5
ANOVA results for exergy efficiency of SCWO Process 3

Source	Sum of squares	df	Mean square	*F*-value	*P*-value
Model	0.0439	9	0.0049	35,003.71	<0.0001
A-Temperature	0.0297	1	0.0297	2.131E5	<0.0001
B-Pressure	1.648E-7	1	1.648E-7	1.18	0.3127
C-EOC	0.0002	1	0.0002	1,524.61	<0.0001
AB	4.219E-7	1	4.219E-7	3.03	0.1253
AC	6.074E-7	1	6.074E-7	4.36	0.0752
BC	3.553E-8	1	3.553E-8	0.2551	0.6290
A^2	0.0139	1	0.0139	99,740.26	<0.0001
B^2	6.677E-7	1	6.677E-7	4.79	0.0647
C^2	1.63E-8	1	1.63E-8	0.1170	0.7423
Residual	9.749E-7	7	1.393E-7		
Lack of fit	9.749E-7	3	3.25E-7		
Pure error	0.0000	4	0.0000		

R^2 = 1; Adeq. precision = 461.6014; Adjusted R^2 = 0.9999; Predicted R^2 = 0.9996; CV = 0.1127%; SD = 0.0004.

Table 6
ANOVA results for exergy efficiency of SCWO Process 4

Source	Sum of squares	df	Mean square	*F*-value	*P*-value
Model	0.0411	9	0.0046	1.654E5	<0.0001
A-Temperature	0.028	1	0.028	1.012E6	<0.0001
B-Pressure	0.0001	1	0.0001	2568.23	<0.0001
C-EOC	0.0001	1	0.0001	2728.55	<0.0001
AB	3.93E-7	1	3.93E-7	14.23	0.007
AC	2.607E-8	1	2.607E-8	0.9439	0.3636
BC	3.476E-9	1	3.476E-9	0.1259	0.7332
A^2	0.0129	1	0.0129	4.685E5	<0.0001
B^2	2.958E-7	1	2.958E-7	10.71	0.0136
C^2	4.405E-9	1	4.405E-9	0.1595	0.7015
Residual	1.933E-7	7	2.762E-8		
Lack of fit	1.933E-7	3	6.444E-8		
Pure error	0.0000	4	0.0000		

R^2 = 1; Adeq. precision = 979.9313; Adjusted R^2 = 1; Predicted R^2 = 0.9999; CV = 0.0755%; SD = 0.0002.

excess oxygen coefficient were all the significant variables for the response with the small '*P*-value', which had an influence on the exergy efficiency.

Adequate precision is an indicator of signal to noise ratio and a ratio greater than 4 is desirable. The ratio of 39.06, 65.66, 461.6 and 979.93 have indicated an adequate signal for the responses of SCWO Processes 1–4, respectively. It represents the model used to navigate the design space. The plot of residuals of four responses are show in Fig. 9. It can be found that the residuals of regression analysis of four response functions follow normal distribution. The points on the residual normal graph were all close to the straight line, which indicated the accuracy of the models, as well as the independence of the residuals.

The optimal parameters of SCWO Processes 1–4 were predicted by Derringer's desirability function. Based on all the above results as shown in Table 7, for SCWO Process 1, the exergy efficiency of 38.9% was obtained with the optimum parameters of temperature (572.5°C), pressure (28 MPa) and excess oxygen coefficient (2). For SCWO Process 2, the exergy efficiency of 41.1% was obtained with the optimum parameters of temperature (573°C), pressure (24 MPa) and excess oxygen coefficient (2). For SCWO Process 3, the exergy efficiency of 38% was obtained with the optimum parameters of temperature (576.7°C), pressure (25.4 MPa) and excess oxygen coefficient (1). For SCWO Process 4, the exergy efficiency of 26.8% was obtained with the optimum parameters of temperature (576.8°C), pressure (24 MPa) and excess oxygen coefficient (2). And the SCWO Process 2 has the highest exergy efficiency among the SCWO four processes.

5.2. Effect of influencing factors on the exergy efficiency of SCWO process

5.2.1. Effect of temperature

As shown in Fig. 10a, c, e, g, the exergy efficiencies of all four processes increase and then decrease with increasing temperature in the range of 500°C to 600°C. The rise of the temperature contributed to the amount of steam which improved the exergy efficiency of the process. However, as the temperature exceeded the turning point temperature,

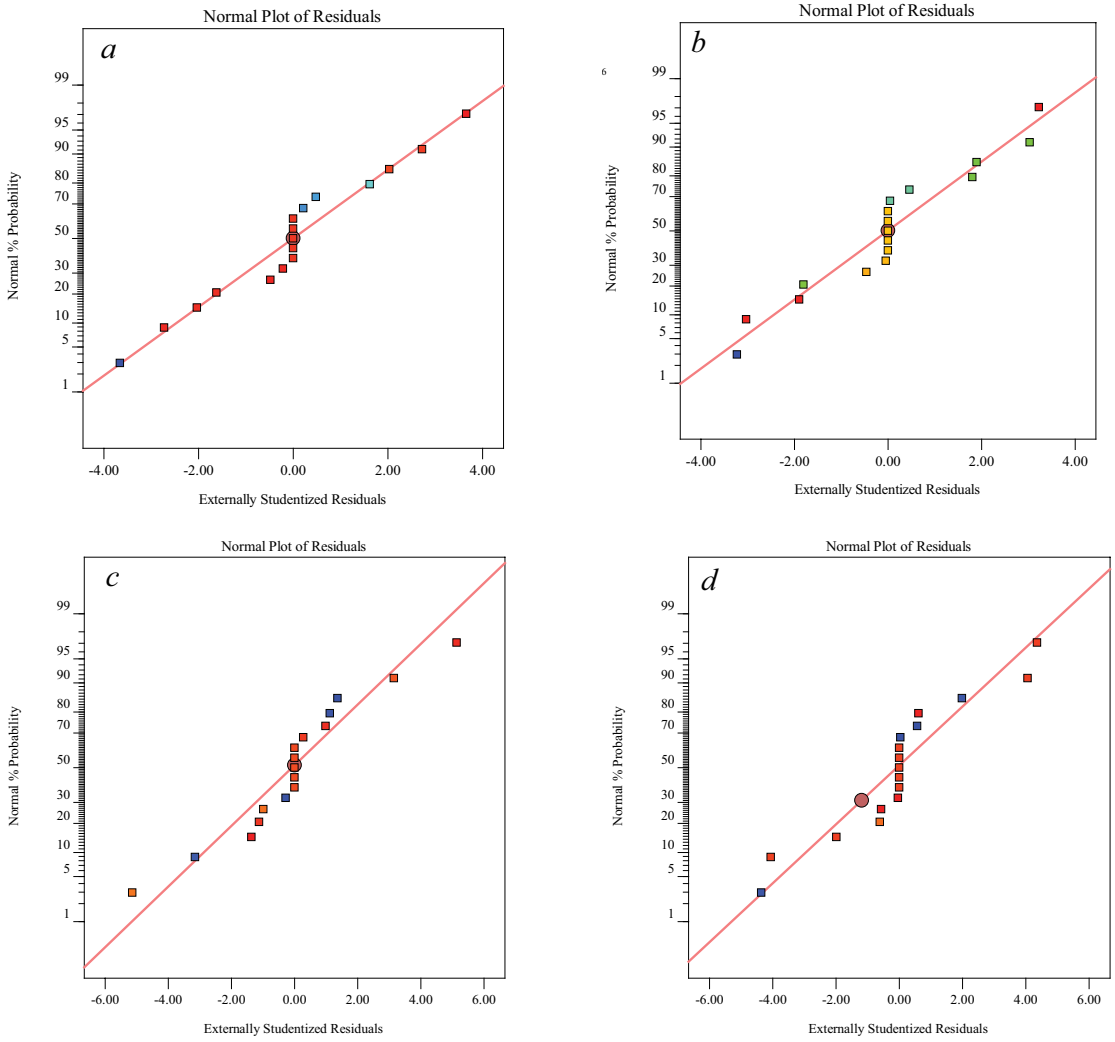

Fig. 9. Normal distribution of residuals in four SCWO processes. (a) Process 1, (b) Process 2, (c) Process 3, and (d) Process 4.

Table 7
Exergy efficiency of four processes

Number	Temperature (°C)	Pressure (MPa)	Excess oxygen coefficient	Exergy efficiency
SCWO Process 1	572.5	28	2	38.9%
SCWO Process 2	573	24	2	41.1%
SCWO Process 3	576.7	25.4	1	38%
SCWO Process 4	576.8	24	2	26.8%

the heat of reaction was less than the heat required to maintain the reactor temperature and the effluent temperature decreased resulting in low process exergy efficiency.

Due to not considering the cooling factor in the compressor, air was used as oxidant in Process 1 and Process 2, the compressor outlet temperature increased which caused the rise of the reactor product temperature. The liquid oxygen was used as the oxidant in Process 3 and Process 4 and absorbed a large amount of reaction heat which reduces the temperature of effluents. Compared with Process 1 and Process 2, the exergy efficiencies of Process 3 and Process 4 are less. Since the exergy efficiency of the turbine varied less than that of the steam generator, the exergy efficiency of Process 2 varied considerably compared to Process 1 but tended to flatten out as the temperature increased. And the exergy efficiency of Process 2 was always greater than that of Process 1. Therefore, the turbine was used to improve the exergy efficiency in the high-temperature effluent process. The trend of exergy efficiency with temperature was similar for Process 3 and Process 4. However, both the exergy efficiency and exergy efficiency variation were smaller for Process 4 than for Process 3. Therefore, the steam generator was more suitable than turbine for obtaining higher exergy efficiency in low-temperature effluent processes.

5.2.2. Effect of pressure

As the pressure was in the range of 24 to 28 MPa, the exergy efficiencies of the four processes remain constant, but the pressure interacted with the temperature and excess oxygen coefficient, as shown in Figs. 10 and 11. In Process 1, the temperature-excess oxygen coefficient contour shifted downward as the pressure increased, while the contour for Process 2 shifted in the opposite trend. In Process 3, the temperature-excess oxygen coefficient contour showed a trend of increasing and then decreasing with increasing pressure, and the trend of the contour moving in Process 4 was the same as that in Process 2. This was mainly due to the fact that higher pressure was beneficial to improve the efficiency of the steam generator, but higher pressure will increase the power consumption of the compressor and pump, which will also had a negative impact on the exergy efficiency of the turbine.

5.2.3. Effect of excess oxygen coefficient

As shown in Fig. 10b, d, f, h, the exergy efficiencies of Process 1, Process 2 and Process 4 gradually increased while the exergy efficiency of Process 3 gradually decreased with excess oxygen coefficient in the range of 1–2. When the oxidizer was air, as in Process 1 and Process 2, the increase in the excess oxygen coefficient contributed to improve steam generation which improved the exergy efficiency of the process. In Process 2, the increase in the excess oxygen coefficient contributed to power generation which also benefited the process exergy efficiency. When the oxidant was liquid oxygen, as in Process 3, the increase in the excess oxygen coefficient substantially raised the heat required to maintain the reactor temperature which was not conducive to improving the process exergy efficiency. However, in Process 4, the increase in the excess oxygen coefficient increased the turbine power generation which positively affected the process exergy efficiency.

6. Economic viability studies

6.1. Capital requirement

The economic viability study was to minimize the total cost of the SCWO system by analyzing the capital requirement and equipment cost of the wastewater requirement SCWO process and provide reference for the industrialization of the SCWO process. The capital requirement and equipment cost of the four processes were shown in Fig. 12. All equipment costs in processes were calculated by economic model [30]. The Chemical Economic Device Cost Index (CEPCI) [31] was used to indicate capital demand in this paper. The capital requirements of the four SCWO processes at the highest exergy efficiency were shown in Table 8, respectively. The order of capital requirement from high to low is Process 2, Process 1, Process 4 and Process 3. The three components with the highest capital requirement are compressor, reactor and plunger pump in Process 1. The three components with the highest capital requirement are compressor, high-pressure gas–liquid separator and reactor in Process 2. The three components with the highest capital requirement are plunger pump, reactor and vapor generator in Process 3. The three components with the highest capital requirement are plunger pump, reactor and turbine in Process 4. Comparing the economic models of the four processes, the capital requirement of Process 1 and Process 2 is higher than others. It is mainly due to the high amount of nitrogen resulting in higher capital requirements of the reactor and compressor. The equipment cost of liquid oxygen pump and reactor in Process 3 and Process 4 are low. The capital requirement of steam generator in Process 1 is higher than in Process 2. The capital requirement of steam generator in Process 3 is also higher than in Process 4. The capital requirement of the high-pressure gas–liquid separator, low pressure gas–liquid separator and turbine is higher in Processes 2 and 4 than in

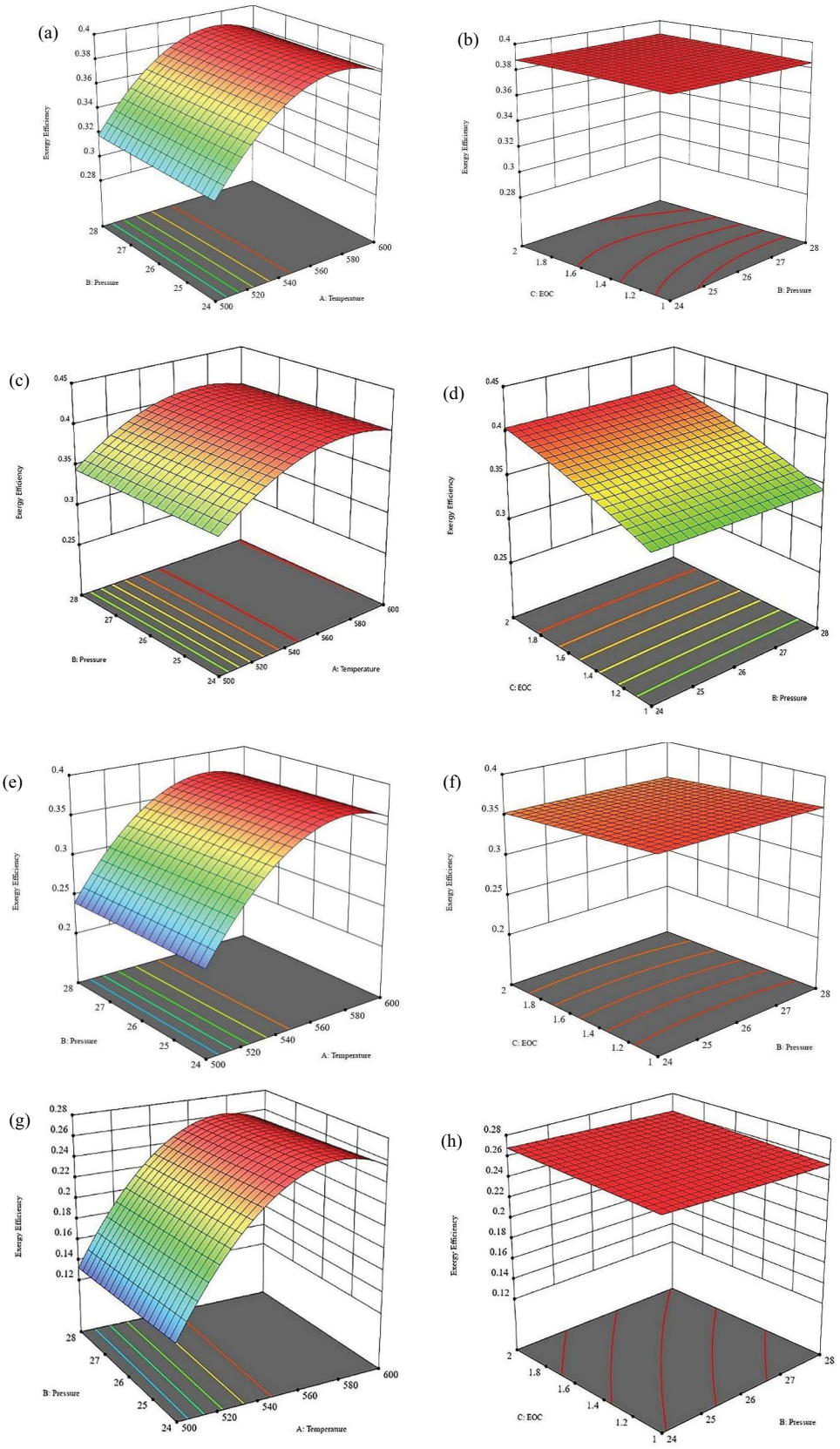

Fig. 10. 3D response surface of interactive effect of (A) temperature and (B) pressure in four processes: (a) Process 1, (c) Process 2, (e) Process 3, (g) Process 4. 3D response surface of interactive effect of (B) pressure and (C) excess oxygen coefficient in four processes: (b) Process 1, (d) Process 2, (f) Process 3, and (h) Process 4.

Table 8
Capital requirement of the process ($)

Equipment	Process 1	Process 2	Process 3	Process 4
Plunger pump	667,103	612,673	632,156	612,673
Compressor	3,333,192	3,251,366	–	–
Liquid oxygen pump	–	–	190,052	361,751
Reactor	738,383	2,075,715.5	551,444	594,900
Preheater	51,938	5,620	75,523	5,742
Vapor generator	334,719	251,759	402,736	154,797
High pressure separator	–	2,746,253	–	255,044.5
Low pressure separator	–	456,150.5	–	14,485
Turbine	–	2,037,723	–	554,258
Storage tank	–	0	4,744	7,042
Total cost	5,125,336	9,195,765	1,856,655	2,560,692

Table 9
Operating cost of the process ($)

Parameter	Process 1	Process 2	Process 3	Process 4
Material cost	0	0	32.32	64.63
Power consumption	2,247,720	2,121,336	90,599	94,209
Maintenance cost	256,266.8	459,788.25	92,832	128,034.6
Depreciation cost	246,016.13	441,396.72	89,119.44	122,913.216
Labor cost	8,357.94	8,357.94	8,357.94	8,357.94
Steam benefit	1,099,437	761,041	515,036	306,101
Electrical energy	0	268,518	0	38,212
Total cost	1,659,823	17,332,803	–1,444.21	436,354

Table 10
Four process evaluation parameters

Evaluation index	Process 1	Process 2	Process 3	Process 4
Exergy efficiency (%)	38.9	41.1	38	26.8
Cost ($)	6,785,159	26,528,568	1,855,210.79	2,997,046

Processes 1 and 3, respectively. The capital requirement of the gas–liquid separator in Process 2 is higher than in Process 4 due to air used as the oxidant in Process 2. Although the capital requirement of liquid oxygen tank is added in Process 3 and Process 4, it accounts as a small percentage.

6.2. Equipment cost

It is assumed that processes work 300 days a year, 24 hours a day. The operating cost is mainly composed of annual capital demand, oxidant cost, power consumption, high pressure steam revenue and turbine power. Assume that the SCWO plant life is 20 years. The net residual value rate of equipment is 4%. The depreciation period is 20 years. The depreciation rate is 4.8% and the annual maintenance cost is 5%. As shown in Table 9, the operating costs of the four processes from high to low are Process 2, Process 1, Process 4, and Process 3. The maintenance and depreciation costs of all four processes are high. The energy consumption of compressor in Process 1 and Process 2 are greater than that of liquid oxygen pump in Process 3 and Process 4. The steam recovery amount of the four processes from high to low is Process 1, Process 2, Process 3 and Process 4 and the revenue of the four processes from high to low is Process 1, Process 2, Process 3 and Process 4.

7. Comprehensive analysis

The exergy efficiency and total costs of the four processes were shown in Table 10. Combined with the exergy efficiency and economic analysis, exergy efficiency in Process 2 is the highest among them. The cost in Process 2 are 3.9 and 14.3 times higher than in Process 1 and 3, respectively. The exergy efficiency in Process 4 is the lowest compared to the others which is not beneficial for high-temperature effluent heat and pressure energy recovery. The exergy efficiencies in Process 1 and Process 3 are 38.9% and 38%, respectively while the total cost in Process 1 is 3.66 times

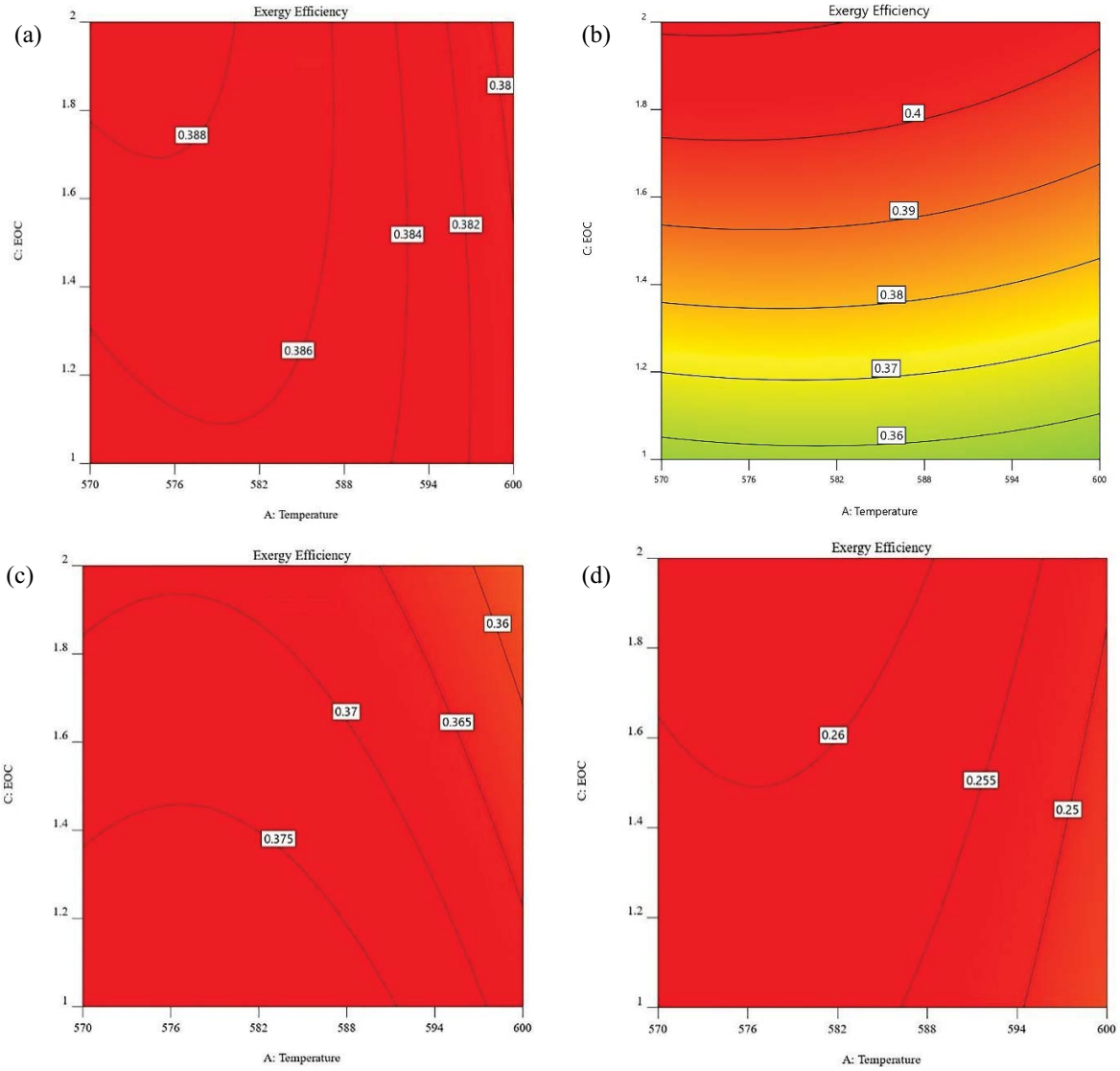

Fig. 11. Temperature (A)-excess oxygen coefficient (B) contour for the four processes (a) Process 1, (b) Process 2, (c) Process 3, and (d) Process 4.

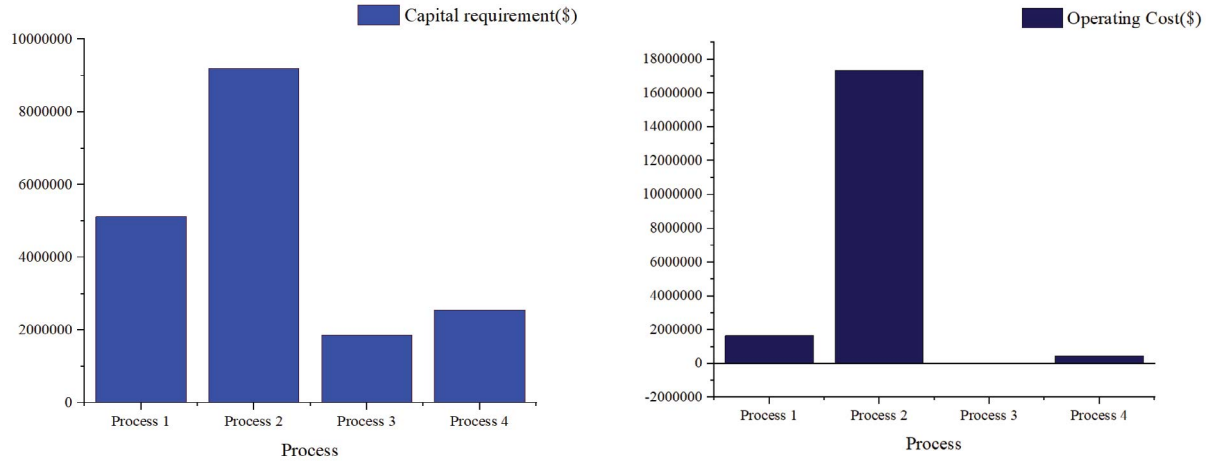

Fig. 12. Capital requirement and equipment cost of the four processes.

higher than in Process 3. The reaction pressure in Process 1 is higher than in Process 3 resulting in the decrease in safety and the increase of the difficulties in processing and manufacturing. The liquid oxygen reacts rapidly with organic wastewater after gasification in the SCWO reactor and reduces the reaction time. Meanwhile, the liquid oxygen at the reaction zone outer layer absorb heat and produce a low-temperature gas film layer, which reduces the temperature of the metal bearing wall and reduces corrosion. The SCWO high temperature product heat energy exergy efficiency is higher than the pressure energy, and the work done by pressure energy is limited. Thermal energy recovery is more suitable for SCWO processes.

8. Conclusion

Through the analysis of four wastewater treatment SCWO processes, the most significant factor influencing the process exergy efficiency is temperature following by the excess oxygen coefficient and pressure. The exergy efficiency in processes from high to low are Process 2, Process 1, Process 3 and Process 4. The air was used as oxidant in Process 2 and Process 1 where the high-pressure energy recovery was used in Process 2. Liquid oxygen was used as the oxidant in Process 3 and Process 4, where high pressure energy recovery was used in Process 4. Exergy efficiency in Process 1, Process 2 and Process 3 are approximately equal. The exergy efficiency in Process 4 is significantly lower than other processes. Total cost from high to low is Process 2, Process 1, Process 4 and Process 3 and the cost in Process 2 is significantly higher than the other processes.

The SCWO process has higher exergy efficiency and cost with air as the oxidant. The SCWO process exergy efficiency is higher when by-product steam is the energy recovery method process. The effect of liquid oxygen and air on the process exergy efficiency is same when the excess oxygen coefficient is 1. Therefore, the SCWO process is suitable for the industrial development of SCWO technology with liquid oxygen as the oxidant and by-product steam as the energy recovery process.

Compared with other processes, Process 3 has advantages of high exergy efficiency, economy and safety, which is suitable as the process of supercritical water oxidation. The exergy efficiency in Process 3 obtained the maximum value of 38% at temperature (576.7 K), excess oxygen coefficient (1) and pressure (25.4 MPa). And the analysis of Process 3 economic evaluation showed total cost, capital requirement and operating cost of $1,855,210.79, $1,856,655 and $–1,444.21, respectively.

References

[1] P. Feng, W.P. Yang, D.H. Xu, M.Y. Ma, Y. Guo, Z.F. Jing, Characteristics, mechanisms and measurement methods of dissolution and deposition of inorganic salts in sub-/supercritical water, Water Res., 225 (2022) 119167, doi: 10.1016/j.watres.2022.119167.

[2] T.T. Xu, S.Z. Wang, Y.H. Li, J.N. Li, J.J. Cai, Y.S. Zhang, D.H. Xu, J. Zhang, Review of the destruction of organic radioactive wastes by supercritical water oxidation, Sci. Total Environ., 799 (2021) 149396, doi: 10.1016/j.scitotenv.2021.149396.

[3] P. Parthenidis, E. Evgenidou, D. Lambropoulou, Wet and supercritical oxidation for landfill leachate treatment: a short review, J. Environ. Chem. Eng., 10 (2022) 107837, doi: 10.1016/j.jece.2022.107837.

[4] Z. Chen, H.Z. Chen, X.L. Liu, C.L. He, D.T. Yue, Y.J. Xu, An inclined plug-flow reactor design for supercritical water oxidation, Chem. Eng. J., 343 (2018) 351–361.

[5] W. Liao, Q.W. Zhao, H.J. Chen, C.H. Liao, Y.F. Wang, X.J. Wang, Experimental investigation and simulation optimization of a pilot-scale supercritical water oxidation system, Energy Convers. Manage., 199 (2019) 111965, doi: 10.1016/j.enconman.2019.111965.

[6] M. Belén García-Jarana, P. Casademont, J. Sánchez-Oneto, J.R. Portela, E.J. Martínez de la Ossa, Hybridization of supercritical water oxidation and gasification processes at pilot plant scale, J. Supercrit. Fluids, 186 (2022) 105609, doi: 10.1016/j.supflu.2022.105609.

[7] D.H. Xu, S.Z. Wang, X.Y. Tang, Y.M. Gong, Y. Guo, Y.Z. Wang, J. Zhang, Design of the first pilot scale plant of China for supercritical water oxidation of sewage sludge, Chem. Eng. Res. Des., 90 (2012) 288–297.

[8] J.Q. Yang, S.Z. Wang, Y.H. Li, Y. Zhang, D.H. Xu, Novel design concept for a commercial-scale plant for supercritical water oxidation of industrial and sewage sludge, J. Environ. Manage., 233 (2019) 131–140.

[9] F.M. Zhang, Y.F. Li, Z.J. Liang, T. Wu, Energy conversion and utilization in supercritical water oxidation systems: a review, Biomass Bioenergy, 156 (2022) 106322, doi: 10.1016/j.biombioe.2021.106322.

[10] L.L. Qian, S.Z. Wang, M.M. Ren, S. Wang, Co-oxidation effects and mechanisms between sludge and alcohols (methanol, ethanol and isopropanol) in supercritical water, Chem. Eng. J., 366 (2019) 223–234.

[11] W.P. Yang, D.H. Xu, H. Wang, X.H. Gong Y. Wei, Y. Wang, Supercritical water oxidation of coal pyrolysis wastewater: effects of main operating parameters and reaction pathways of 2-(N-Morpholino)ethanesulfonic acid, Fuel, 322 (2022) 124261, doi: 10.1016/j.fuel.2022.124261.

[12] A. Leybros, A. Roubaud, P. Guichardon, O. Boutin, Ion exchange resins destruction in a stirred supercritical water oxidation reactor, J. Supercrit. Fluids, 51 (2010) 369–375.

[13] O.N. Fedyaeva, S.V. Morozov, A.A. Vostrikov, Supercritical water oxidation of chlorinated waste from pulp and paper mill, Chemosphere, 283 (2021) 131239, doi: 10.1016/j.chemosphere.2021.131239.

[14] O.N. Fedyaeva, V.R. Antipenko, A.A. Vostrikov, Heavy oil upgrading at oxidation of activated carbon by supercritical water-oxygen fluid, J. Supercrit. Fluids, 126 (2017) 55–64.

[15] J.P.S. Queiroz, M.D. Bermejo, F. Mato, M.J. Cocero, Supercritical water oxidation with hydrothermal flame as internal heat source: efficient and clean energy production from waste, J. Supercrit. Fluids, 96 (2015) 103–113.

[16] Q.H. Yan, Y.W. Hou, J.R. Luo H.J. Miao, H. Zhang, The exergy release mechanism and exergy analysis for coal oxidation in supercritical water atmosphere and a power generation system based on the new technology, Energy Convers. Manage., 129 (2016) 122–130.

[17] S.H. Guo, C.Y.F. Ren, Y. Wang S. Liu, M.M. Du, Y.N. Chen, L.J. Chen, Thermodynamic modeling and analysis of the heat integration and power generation in pig manure supercritical water gasification system, Energy Convers. Manage., 248 (2021) 114809, doi: 10.1016/j.enconman.2021.114809.

[18] M.D. Bermejo, M.J. Cocero, F. Fernandez-Polanco, A process for generating power from the oxidation of coal in supercritical water, Fuel, 83 (2004) 195–204.

[19] F. Marias, F. Mancini, F. Cansell, Mercadier, Energy recovery in supercritical water oxidation process, Environ. Eng. Sci., 25 (2008) 123–130.

[20] Y.F. Huang, F.M. Zhang, Z.J. Liang, T. Wu, Effect of hydrothermal flame generation methods on energy consumption and economic performance of supercritical water oxidation systems, Energy, 266 (2023) 126452, doi: 10.1016/j.energy.2022.126452.

[21] F. Zhang, B.Y. Shen, C.J. Su, C.Y. Xu, J.N. Ma, Y. Xiong, C.Y. Ma, Energy consumption and exergy analyses of a supercritical

water oxidation system with a transpiring wall reactor, Energy Convers. Manage., 145 (2017) 82–92.
[22] J.M. Liang, Y. Liu, J.W. Chen, J.Q. E, E. Leng, F. Zhang, G.L. Liao, Performance comparison of black liquor gasification and oxidation in supercritical water from thermodynamic, environmental, and techno-economic perspectives, Fuel, 334 (2023) 126787, doi: 10.1016/j.fuel.2022.126787.
[23] C.C. Luo, H. Xi, Y.Q. Feng, Z.C. Hung, Performance evaluation of a supercritical water oxidation cogeneration system using hydrogen peroxide as oxidant, Energy Convers. Manage., 267 (2022) 115914, doi: 10.1016/j.enconman.2022.115914.
[24] P. Sharan, S.K. Thengane, T.J. Yoon, J.C. Lewis, R. Singh, R.P. Currier, A.T. Findikoglu, A novel approach for produced water treatment: supercritical water oxidation and desalination, Desalination, 532 (2022) 115716, doi: 10.1016/j.desal.2022.115716.
[25] H.S. Li, S.Q. Zhou, Y.B. Sun, J. Lv, Application of response surface methodology to the advanced treatment of biologically stabilized landfill leachate using Fenton's reagent, Waste Manage., 30 (2010) 2122–2129.
[26] J.L. Chen, H.F. Chen, F.M. Zhang, Z.Y. Chen, C.J. Su, Simulation and economic analysis of supercritical water oxidation system based on nitrogen protective film, Environ. Eng., 37 (2019) 61–66.
[27] H. Xi, M.J. Li, Z.H. Huang, M.W. Wang, Energy, exergy and economic analyses and performance assessment of a trigeneration system for power, freshwater and heat based on supercritical water oxidation and organic Rankine cycle, Energy Convers. Manage., 243 (2021) 114395, doi: 10.1016/j.enconman.2021.114395.
[28] N. Segond, Y. Matsumura, K. Yamamoto, Determination of ammonia oxidation rate in sub- and supercritical water, Ind. Eng. Chem., 41 (2022) 6020–6027.
[29] F.M. Zhang, Y.X. Ding, C.J. Su, Z.Y. Chen, Energy self-sufficiency of a supercritical water oxidation system with an improved cooled-wall reactor for power generation, Appl. Therm. Eng., 172 (2020) 115158, doi: 10.1016/j.applthermaleng.2020.115158.
[30] R. Smith, Chemical Process Design and Integration, John Wiley & Sons Ltd., Chichester, 2005.
[31] C. Maxwell, Cost Indices, 2021.